1 Melting function

The noble gases concentration in the residual, melt-depleted mantle depends on the mineral-melt partition coefficient, D, and enters via the melt function, $f = C_r/C_0$, where C_r is the concentration in the residual mantle and C_0 the concentration prior to melting. f is the fraction of noble gas left in the residual mantle, whereas the remainder is in the melt phase, which solidifies to form ocean crust. In our analysis it is assumed that all noble gases are lost from the ocean crust by the time it is subducted back into the mantle. We thus assume that a fraction f of the noble gases are lost to the Earth's oceans and atmosphere upon partial melting of a given mass of mantle. The relation between D and f is shown in Figure S1. Fractional and batch melting are end-member cases of the more general dynamic melting model with melt retention [32], where C_m, the concentration in the melt, is given by

$$C_m = C_{m,0} \left(\frac{D + \alpha - F(D + \alpha)}{D + \alpha - f_p(D + a)} \right)^{((1-D)/(D+\alpha))} . \qquad (1)$$

Here $\alpha = f_p/(1 - f_p)$, f_p is retained melt fraction, C_0 is the concentration in the solid prior to melting and $C_{m,0}$ is defined as

$$C_{m,0} = C_0 (D + f_p(1 - D)). \qquad (2)$$

The two end-member cases are fractional ($f_p = 0$) and batch ($f_p = F$) melting, where F is the melt fraction. For fractional melting

$$f = (1 - F)^{1/D - 1} \qquad (3)$$

and for batch melting

$$f = D(D + F - DF)^{-1}. \qquad (4)$$

A reasonable upper limit for the fraction of retained melt is 2%, or $f_p = 0.02$. For our model calculations we therefore assume a melt retention of $f_p = 0.02$ with partition coefficients of $D_{He} = 0.0002$ and $D_{Ar} = 0.0011$ [12]. Figure S1 shows that for $D_{He} \approx 0.0002$ essentially all He is lost from the mantle residue upon melting and the same holds true for Argon (Ar) at $D_{Ar} \approx 0.001$. Although recent estimates for He mineral-melt partition coefficients differ by about one order of magnitude, high estimates of $D_{He} = 0.0025 - 0.006$ [33] still result in at least 99% of He loss from the mantle under typical melting regimes, as shown in Figure S1. Because for any reasonable choice of D_{He}, D_{Ar} and melt fraction F, the value f is small, our model results are not sensitive to the particular choice of f_p or D. This assertion is substantiated,
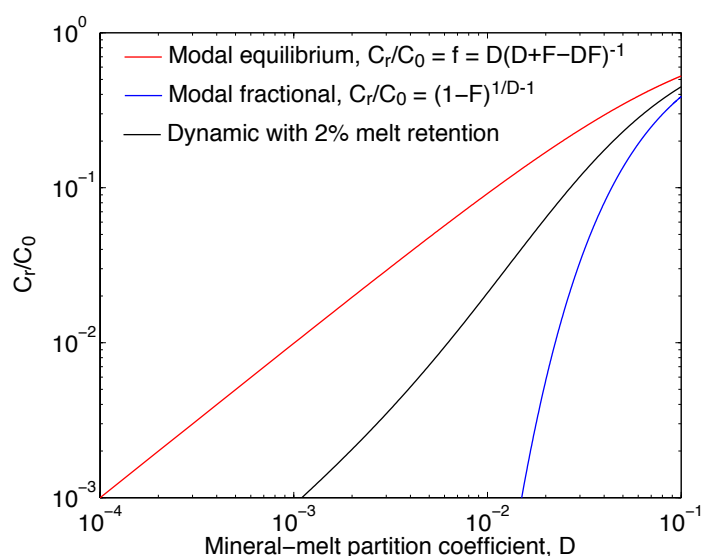
Figure S 1: C_r/C_0 for the residual mantle after partial melting, assuming $F = 0.1$. C_r/C_0 is essentially zero for any reasonable values of D.

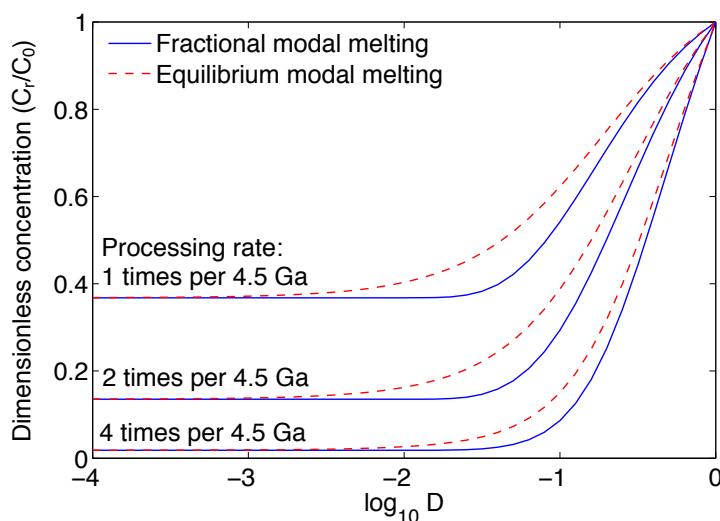for example, for the case of instantaneous mixing given by Equation (1) and shown in Figure S2.

Figure S2: C_r/C_0 after 4.5 Ga as a function of D for different values of N, the reservoir masses processed over 4.5 Ga, with and $F = 0.1$ and assuming instantaneous mixing. Here, C_r is the concentration of a non-radiogenic, non-recycled noble gas in the mixed mantle reservoir after 4.5 Ga of mantle processing and C_0 is the initial concentration. Note that the extent of outgassing asymptotically approaches $D = 0$ and is essentially constant for $D < 0.01$.

2   Mass of unmixed recycled slab

Equation (7) in the Methods section gives the fraction of the mantle reservoir comprised by segregated (unmixed) recycled slab (M_S/M_0). Figure (S3) shows the value of M_S/M_0 as a function of reservoir masses processed over 4.5 Ga for different values of τ. Unless a mantle reservoir is predominantly comprised of unmixed slab, τ cannot exceed a few Ga (at least in a time-averaged sense), if the mantle reservoir has been processed at least once over Earth's history (i.e., $N \geq 1$).
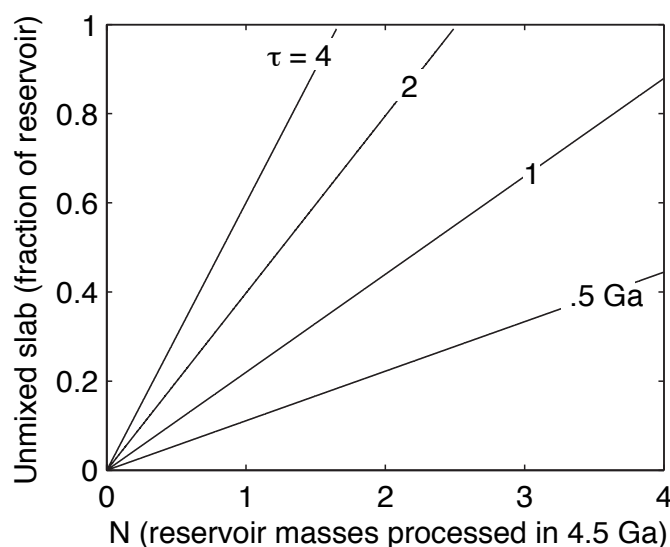
Figure S3: The fraction of segregated slab, M_S/M_0 after 4.5 Ga as a function of N for different values of τ.

3   Description of the geochemical reservoir model

We consider two geochemical mantle reservoirs denoted by subscripts U and L, with masses that are equivalent to the Earth's upper mantle and lower mantle, respectively. At time zero, the reservoirs consist entirely of a well-mixed region with BSE compositions. Recycling and mixing of the slabs into the mantle causes the upper and lower mantle reservoirs to evolve into a

Figure S 4: Schematic diagram of the geochemical reservoir model. Both lower and upper mantle reservoirs are characterized by a well-mixed region and unmixed slabs (Figure 1 of the main text). Reservoir sizes are not drawn to scale. For detailed description see Methods, as well as Section 3 of this Supplemental Information.

mixed region and the unmixed, recycled slabs. The slabs are comprised of ocean crust and residual mantle. At each time step, i, there is a mass flux out from the mixed region of each mantle reservoir with magnitude Q_L and Q_U for lower and upper mantle, respectively. Q_U is processed through partial melting at ridges at a melt fraction F. A fraction of the flux out of the lower mantle, given by $Q_L - Q_P$, mixes directly with the mixed upper mantle, whereas the remainder, Q_P, rises to the surface to undergo partial melting at a melt fraction $F = 0.1$. This flux, Q_P, represents the plume flux from the lower mantle. A fraction, x_P, of residual mantle produced by plume melting mixes directly with the upper mantle and corresponds to a mass flux of $x_P (1 - F) Q_P$. The remainder, $(1 - x_P) (1 - F) Q_P$, becomes part of the oceanic lithosphere, which together with the oceanic crust comprises the slabs. We use the dynamic melting model with 2% melt retention (Section

1) to infer how He, Ar, U, Th, and K will partition between the oceanic crust and residual mantle. The plume melt flux is given by $F\,Q_P$ and is enriched in He, Ar, U, Th and K. We assume that all noble gases are lost from the melt (ocean crust) and are not recycled. A fraction, x_C of U, Th, and K contained in the melt is assumed to be sequestered in the continental crust and thus not recycled to the mantle. The remainder is contained within the ocean crust. Neglecting the actual mass of continental crust produced over time, it is assumed that slab production, given by $F\,Q_P + (1 - x_P)\,(1 - F)\,Q_P + Q_U$, is balanced by slab subduction at a rate of Q_S. In other words, we assume that slabs are subducted at the same rate as they are produced, with the actual time lag between production and subduction implicitly accounted for by the characteristic mixing time, τ. A fraction x_S of subducted slabs enters the lower mantle and mass balance requires that $Q_L = x_S Q_S$. Subducted slabs containing low concentrations of residual He, Ar, U, Th, and K mix with ambient mantle on a characteristic time scale, τ_L and τ_U for lower and upper mantle, respectively. We track the mass balance for ^{3}He, ^{4}He, ^{40}Ar, U, Th and K in the mixed mantle reservoir and in the individual parts of unmixed slab by numerical integration.

To fully understand the range of permissible and realistic parameters and outcomes, we allow a number of parameters to vary independently over a large number of Monte Carlo simulations. The ranges of variable input parameters (summarized in Table S1) are:

- Present day processing rate $Q_{L,present}$ falls within the range of present day plume flux estimates (2×10^{13} to 20×10^{13} kg y^{-1} [27]).

- Present day processing rate $Q_{U,present}$ is equal to present day upper-mantle processing rate through mid-ocean ridges (7×14 kg y^{-1} [34]).

- Q_L is "anchored" at present day values and may vary through time as $Q_L(t) = Q_{L,present} \exp(t/4.5 \text{ Ga})$, so that the entire mass of lower mantle processed over 4.5 Ga ranges from 0.0304 (present day low estimate of plume flux) to 2 lower mantle masses.

- Q_U is "anchored" at present day values and may vary through time as $Q_U(t) = Q_{U,present} \exp(\alpha t/4.5 \text{ Ga})$, so that the entire mass of upper mantle processed over 4.5 Ga ranges from 2.6 (present day upper-mantle processing rate through mid-ocean ridges) to 10 upper mantle masses.

- The residual plume mantle that mixes with upper mantle, x_P, is allowed to vary from 0 to 1, but assumed constant for any given model case.

- The fraction of slabs that subduct into lower mantle is x_S. The value of x_S is allowed to vary randomly for each case, but is always constrained to a value such that $x_S Q_S \geq Q_P$.

- The fraction of U, Th and K that is extracted and stored in the continental crust, x_C, is allowed to vary between 0 and 1 and is given by $x_C(t) = r_1 * \exp(-10^{r_2} t/4.5 \text{ Ga})$, where r_1 is a random number between 0 and 1 and r_2 is a random number between -5 and 5. Both r_1 and r_2 are independent and differ for each Monte Carlo realization.

- The initial (primordial) concentration of ^{3}He in upper and lower mantle falls between 0.75×10^{11} to 1.5×10^{11} atoms g^{-1}.

- Characteristic upper and lower mantle mixing times may vary independently within the range 0-4 Ga.

We thus examine a broad range of parameter space to fully explore the realm of feasible mantle evolution models for a coupled upper-lower mantle system. Constant initial conditions for all simulations are as follows:

- Initial (primordial) ^{3}He/^{4}He $= 120 R_A$ for the entire mantle.

- Initial (primordial) ^{40}Ar $= 0$ for the entire mantle.

- Initial (primordial) mantle concentrations for radioactive elements are based on Bulk Silicate Earth estimates (VanSchmus, 1995) and are ^{238}U $= 40$ ppb, ^{235}U $= 12$ ppb, ^{232}Th $= 95$ ppb and ^{40}K $= 327$ ppb.

From the Monte Carlo realizations we select outcomes that each meet all of the following criteria:

- Present day ^{3}He/^{4}He in the upper mantle $= 8.5 \pm 0.5 R_A$.

- Present day U content of the upper mantle falls within the range of estimated values by Workman and Hart [28] (3.2 ppb) and by Boyet and Carlson [29] (5.4 ppb).

- Present day K content of the upper mantle falls within the range of estimated values by Workman and Hart [28] (50 ppm) and by Boyet and Carlson [29] (68.4 ppm).

- The present day rate of ^{3}He loss from the upper mantle falls within 75-100% of the estimated ^{3}He flux to the oceans (1060 mole y^{-1} [30]).

- Present day ^{40}Ar in the mantle is within 40-60% of radiogenic ^{40}Ar produced over 4.5 Ga within a bulk-slicate Earth (BSE) mantle, assuming K$_{BSE}$ = 235 ppm and zero primordial ^{40}Ar.

Table S1: Parameters used in the geochemical mantle reservoir model

Parameter	Description	Value
M_U	mass of upper mantle	1.1×10^{24} kg
M_L	mass of lower mantle	2.96×10^{24} kg
Q	instantaneous processing rate	$\lesssim 10^{16}$ kg y^{-1}
$Q_{U,present}$	present day processing rate	7×10^{14} kg y^{-1}
$Q_{L,present}$	present day processing rate	$2 - 20 \times 10^{13}$ kg y^{-1}
τ	characteristic mixing time	0-4 Gy
$(^3\text{He}/^4\text{He})_{t=0}$	initial ratio	120 R$_A$
$^3\text{He}_{t=0}$	initial ^{3}He concentration	$0.75 - 1.5 \times 10^{11}$ atoms g^{-1}
$^{40}\text{Ar}_{t=0}$	initial ^{40}Ar concentration	0 ppb
$^{238}\text{U}_{t=0}$	initial ^{238}U concentration	40 ppb [35]
$^{235}\text{U}_{t=0}$	initial ^{235}U concentration	12 ppb [35]
$^{232}\text{Th}_{t=0}$	initial ^{232}Th concentration	95 ppb [35]
$^{40}\text{K}_{t=0}$	initial ^{40}K concentration	327 ppb [35]
D_{He}	mineral-melt partition coefficient	2.0×10^{-4} [12]
D_{Ar}	mineral-melt partition coefficient	1.1×10^{-3} [12]
D_U	mineral-melt partition coefficient	3.0×10^{-3} [36]
D_{Th}	mineral-melt partition coefficient	3.4×10^{-3} [36]
D_K	mineral-melt partition coefficient	2.2×10^{-3} [36]
x_P	frac. residual plume into upper mantle	0 to 1
Q_S	mass flux of subducting slab	$Q_S = Q_L + Q_U$
Q_P	plume flux	$\leq Q_L$
x_S	fraction slab into lower mantle	$x_S Q_S \geq Q_P$
x_C	fraction U, Th, K to continental crust	$x_C(t) = r_1 * \exp(-10^{r_2} \hat{t})$
$\hat{t}$	dimensionless time	$t/(4.5 \times 10^9)$
r_1	random number	0 to 1
r_2	random number	-5 to 5

4 Depletion of the mantle in Samarium and Neodymium

To demonstrate that our model results for noble gases are also consistent with the depleted character of the mixed region of the upper and lower mantle, we present model predictions for the Neodymium (Nd) isotopic evolution (Figure S5). The approach taken for the Samarium-Neodymium isotopic system is identical to our modeling of the radioactive elements U, Th and K. We use initial (bulk silicate Earth) abundances of 1.25 ppm for Nd and 0.406 ppm for Sm [37], as well as partition coefficients of 0.031 and 0.045 for Nd and Sm, respectively [28]. Although we do not model recycling of continental crust explicitly, our model results imply that recycled continental crust in the mantle may comprise approximately 0.5% of the mantle. For model cases that meet all aforementioned noble-gas related constraints, as well as $9 < \varepsilon^{143}\mathrm{Nd} < 10$ for the mixed region of the upper mantle, we find that the mixed lower mantle assemblage with the primitive noble gas signatures ($^{3}\mathrm{He}/^{4}\mathrm{He}$ ratio between 35-40 $\mathrm{R_A}$) has present day $\varepsilon^{143}\mathrm{Nd}$ between 2 and 5. This is within the range for FOZO-A and FOZO-B [38].
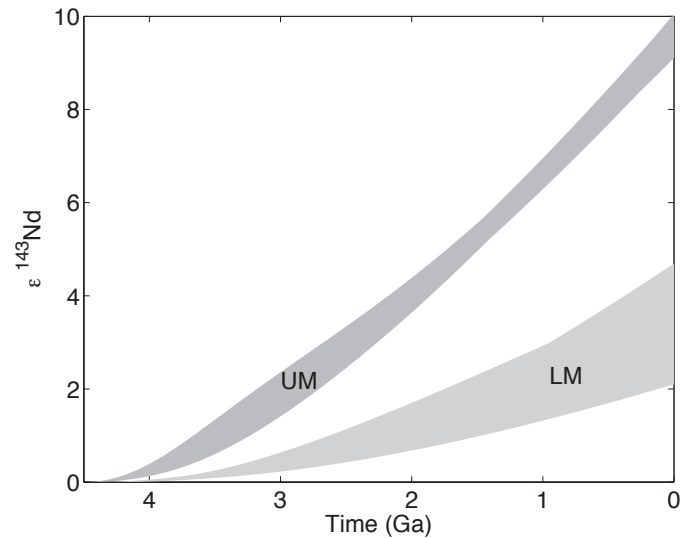
Figure S5: ε^{143}Nd, defined as $([^{143}\text{Nd}/^{144}\text{Nd}]_{\text{sample}}$ / $[^{143}\text{Nd}/^{144}\text{Nd}]_{\text{CHUR}}$ - 1) $\times 10^4$, where CHUR is the Chondritic Uniform Reservoir [39], as a function of time. Shaded areas represent the predicted range of ε^{143}Nd for the mixed portion of the lower mantle (LM) for those model cases that meet all of the aforementioned noble gas observational constraints (i.e., cases shown in Figure 4 of the text) and for which with $9 < \varepsilon^{143}$Nd < 10 in the mixed portion of the upper mantle (UM).

References

[32] Shaw, D. M. Trace elements in magmas. *Cambridge University Press, New York* (2007)

[33] Parman, S. W., Kurz, M. D., Hart, S. R. & Grove, T. L. Helium solubility in olivine and implications for high He-3/He-4 in ocean island basalts. *Nature* **437**, 1140-1143 (2005)

[34] Porcelli, D. & Wasserburg, G. J. Mass-Transfer of Helium, Neon, Argon, and Xenon through a Steady-State Upper-Mantle. *Geochim. Cosmochim. Acta* **59**, 4921-4937 (1995)

[35] Van Schmus, W. R. Natural radioactivity of the crust and mantle. In Ahrens, T. J. (ed.) *Global earth physics: a handbook of physical constants*, 283-291 (The American Geophysical Union, Washingon DC, 1995)

[36] Kelemen, P. B., Rilling, J. L., Parmentier, E. M., Mehl, L. & Hacker, B. R. Thermal Structure due to Solid-State Flow in the Mantle Wedge Beneath Arcs. In Eiler, J. (ed.) *Inside the subduction factory*, 293-311 (American Geophysical Union, Washington, DC, 2003)

[37] McDonough, W. F. & Sun, S.-s.. The composition of the Earth. *Chem. Geol.* **120**, 223-253 (1995)

[38] Jackson, M. G., Kurz, M. D., Hart, S. R. & Workman, R. K. New Samoan lavas from Ofu Island reveal a hemispherically heterogeneous high ^{3}He/^{4}He mantle. *Earth Planet. Sci. Lett.* **264**, 360-374 (2007)

[39] Depaolo, D. J. & Wasserburg, G. J. Nd isotopic variations and petrogenetic models. *Geophys. Res. Lett.* **3**, 249-252 (1976)